

How to Optimize Radiation Dose in Computed Tomography Examinations: Available Methods and Techniques

K. Matsubara¹, H. Kawashima¹, T. Chusin^{2,3}, R. Okubo²

¹Department of Quantum Medical Technology, Faculty of Health Sciences, Institute of Medical, Pharmaceutical and Health Sciences, Kanazawa University, Kanazawa, Japan, ²Department of Quantum Medical Technology, Graduate Course of Medical Science and Technology, Division of Health Sciences, Graduate School of Medical Science, Kanazawa University, Kanazawa, Japan, ³Department of Radiological Technology, Faculty of Allied Health Sciences, Naresuan University, Phitsanulok, Thailand

Abstract— In this review, available methods and techniques for optimizing the radiation dose in computed tomography (CT) examinations are described. Automatic exposure control can adapt tube current according to the patient attenuation needed for achieving a specified image quality by performing tube current modulation (TCM), which allows the tube current to be automatically modulated during the acquisition. TCM is generally divided into the following five types: longitudinal (z-axis), angular (xy-axis), longitudinal and angular (xyz-axis), organ based, and electrocardiogram gated. Optimizing tube voltage is effective for reducing patient dose while maintaining a desired contrast-to-noise ratio. Furthermore, optimization of the reconstruction kernel (including consideration for using an iterative reconstruction), slice thickness of images, bowtie filter, and number of acquisition phases are needed to further optimize the radiation dose. In addition, applications of selective organ shielding (e.g., bismuth shield), dual-energy CT, and newly developed X-ray detection systems may further reduce patient dose.

Keywords— computed tomography, radiation dose, optimization, tube current modulation, iterative reconstruction

I. INTRODUCTION

Computed tomography (CT) is widely used as an essential diagnostic imaging tool in clinics. The introduction of multi-detector CT (MDCT) has increased the number of CT examinations worldwide. However, concern about CT radiation doses has been expressed in the literature [1-3]. Because children are more radiosensitive than adults, potential cancer risks associated with ionizing radiation requires attention, particularly in pediatric CT examinations. Pearce et al. [4] reported that in children, the use of CT with cumulative doses of approximately 50 mGy might almost triple the risk for leukemia and doses of approximately 60 mGy might triple the risk for brain cancer. Mathews et al. [5] also reported that among people aged 0–19 years, the overall cancer incidence was 24% greater for those exposed to radiation than for those unexposed to radiation. Therefore, justifying each CT examination by weighing the benefits against the risks is important.

In addition to justifying each CT examination, radiation doses used should be as low as reasonably achievable (ALARA). To implement ALARA principles in CT image acquisitions, radiologists, physicists, and technologists should make efforts to produce optimal images with the lowest dose to patients; this process is called optimization. Fortunately, CT manufacturers provide various methods and

techniques for optimizing radiation doses in CT examinations. Therefore, radiologists, physicists, and technologists need to be familiar with these methods and techniques.

In this review, we introduce methods and techniques for optimizing the radiation dose in CT examinations. To satisfy the ALARA principle, the dose optimization methods and techniques described in this review should be well understood and appropriately used.

II. TUBE CURRENT MODULATION

Dose, tube current, and exposure time are proportionally related. The noise level is inversely proportional to the square root of tube current (milliamperere, mA) or tube current–time product (milliamperere-second, mAs). An excessive increase in tube current or tube current–time product causes an increase in the patient dose, but excessive tube current reduction can adversely increase image noise levels.

For CT, Brooks and Di Chiro [6] showed the following association between image noise (standard deviation of CT numbers, σ) and patient dose (D):

$$D \propto \frac{e^{-\mu d}}{\sigma^2 \cdot a^2 \cdot b \cdot h} \quad (1)$$

where, μ represents the mean linear attenuation coefficient of the object, d represents the diameter of the object, a represents the sample increment, b represents the sample width, and h represents the slice thickness. Formula (1) is known as Brooks' formula and shows that patient dose and image noise are inversely related to each other.

Although a CT operator must consider patient size when selecting the tube current, adjusting the tube current immediately and appropriately according to the patient size is difficult. In addition, the tube current should be optimized for the thickest or highly attenuated part of the patient when using a fixed tube current, leading to excessive exposure in other parts of the patient.

Automatic exposure control (AEC) is implemented on CT to adapt the tube current according to the patient attenuation needed to achieve a specified image quality using the tube current modulation (TCM) technique. TCM allows the tube current to be automatically modulated during acquisition, and there is no doubt that TCM is effective in optimizing patient dose in CT. Although dose

modulation techniques vary among vendors, they are generally divided into the following five modulation types: longitudinal (z-axis), angular (xy-axis), longitudinal and angular (xyz-axis), organ based, and electrocardiogram (ECG) gated.

A. Longitudinal (z-axis) modulation

In longitudinal modulation, the tube current is adjusted according to the size and anatomical regions of patients. This modulation is performed to produce relatively uniform noise levels through the entire acquisition range. The tube current is modulated to provide the desired image quality at the chosen attenuation on the basis of prior calculations from a localizer radiograph.

Examples of longitudinal dose modulation for thoracic CT for a female RANDO phantom (RAN110; The Phantom Laboratory, Salem, NY, USA) among manufacturers are shown in Fig. 1. Although the tube current is modulated across various anatomical regions, the characteristics of dose modulation vary among manufacturers. Operators should understand that longitudinal modulation that uses data obtained from localizer radiographs cannot appropriately adjust the tube current if the patient is not positioned at the isocenter of the CT gantry [7].

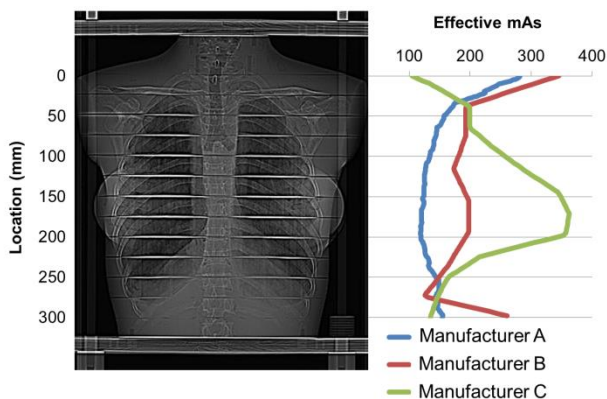


Fig. 1 Comparison of the tube current when applying longitudinal modulation among manufacturers

B. Angular (xy-axis) modulation

X-ray is attenuated more in the lateral direction than in the anteroposterior direction; thus, it is effective that the tube current is modulated within one gantry rotation. The tube current is adjusted according to the attenuation data from the localizer radiograph or in near-real time according to the measured attenuation from the previous 180° projection.

Examples of angular modulations are shown in Fig. 2. These profiles were acquired using the AEC system CARE Dose 4D (Siemens Healthineer, Erlangen, Germany), semiconductor detector CT Dose Profiler (RTI Electronics, Mölndal, Sweden), and custom-made elliptical polymethyl

methacrylate phantoms, measuring 180 × 260 mm (small) and 260 × 380 mm (large) in diameter (Fig. 3), when helical CT acquisitions were performed with and without angular modulation. The semiconductor detector was inserted in the center of the phantom, and time series data of the absorbed dose rate were acquired. With both phantom sizes, the absorbed dose rates were relatively similar between the fixed tube current (FTC) and TCM in the first two cycles. After the first two cycles, the absorbed dose rates stabilized, with only slight fluctuations when TCM was used. These fluctuations were smaller than those with FTC, irrespective of the phantom size.

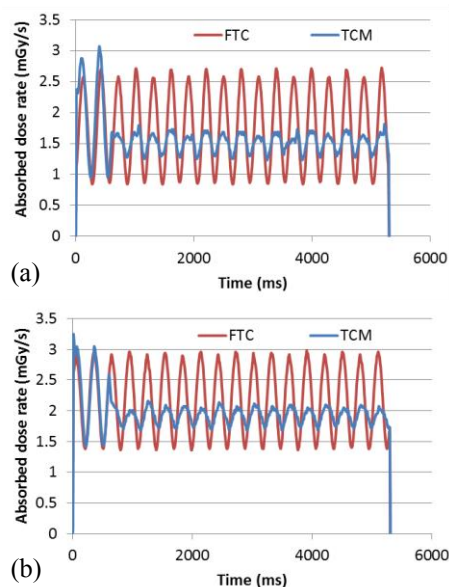


Fig. 2 Examples of absorbed dose rate profiles at the centers of elliptical phantoms with and without angular modulation: (a) absorbed dose rate profiles for a large phantom, (b) absorbed dose rate profiles for a small phantom



Fig. 3 Custom-made small (right) and large (left) elliptical polymethyl methacrylate phantoms. They can be used by inserting a commercially available 16-cm CT dose phantom into these phantoms

C. Longitudinal and angular (xyz-axis) modulation

The simultaneous combination of longitudinal and angular modulations involves the variation of tube current along both the longitudinal (z-axis) and in-plane (xy-axis) directions of a patient. This modulation is the most

comprehensive approach for reducing CT dose because the dose is adjusted according to patient-specific attenuations in all three planes.

D. Organ-based modulation

Organ-based modulation is used for reducing the dose in radiosensitive organs such as the breast, thyroid, and eye lens. In this technique, the tube current is decreased over radiosensitive organs.

One study demonstrated that for thoracic CT, organ-based modulation reduced the absorbed dose in the breast by approximately 22%, without changing CT values and noise levels, relative to those of the reference [8]. The noise levels do not change because the tube current is increased during the remaining acquisition range. Exposure to multiple diagnostic radiographic examinations during childhood and adolescence increases the risk for breast cancer among women with scoliosis [9]. Therefore, organ-based modulation is also preferable for specific patient groups such as children and young women for whom the risk for breast cancer might be increased by thoracic CT.

The International Commission on Radiological Protection revised the occupational equivalent dose limit for eye lens from 150 mSv/y to 100 mSv/5y (no single year exceeding 50 mSv). Patient dose, in addition to occupational dose, for eye lens should be reduced, and organ-based modulation is preferable for reducing the equivalent dose for eye lens during head CT [10]. An example of surface absorbed doses within a single section of the head RANDO phantom (RAN110; The Phantom Laboratory) with and without organ-based modulation (X-CARE; Siemens Healthineer) using standard parameters for head CT is shown in Fig. 4. The results showed that anterior surface doses were lower with organ-based modulation than without it.

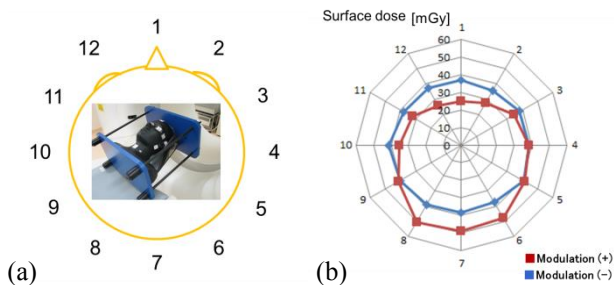


Fig. 4 An example of surface absorbed doses within a single section of the head phantom with and without organ-based modulation: (a) phantom and locations for measuring surface absorbed doses and (b) surface absorbed doses with and without organ-based modulation

E. ECG-gated modulation

In this modulation, a standard tube current is applied over a limited range of heart phases to ensure low noise levels during the phase while minimizing the tube current during the remaining heart phases to reduce the patient dose.

Another type of ECG-gated modulation is to employ prospective gating axial acquisitions in which X-rays are turned on only during a limited heart phase and are completely turned off during other heart phases. However, this method can only be used for patients with low and stable heart rates. Different types of ECG-gated modulation are shown in Fig. 5.

One study demonstrated that in retrospectively ECG-gated helical acquisitions, ECG-gated modulation reduces 3.4–9.2% of the doses absorbed by thoracic organs compared with the reference dose and that in prospectively ECG-gated axial acquisitions, the modulation reduces 66.1–71.0% of the doses absorbed by thoracic organs [11].

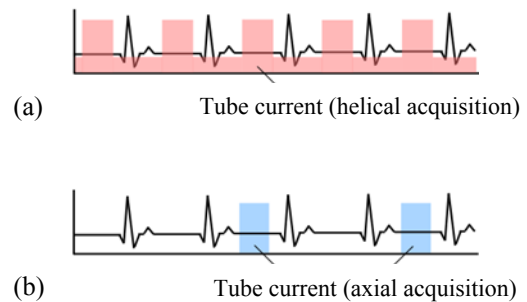


Fig. 5 Different types of ECG-gated modulation: (a) retrospective gating and (b) prospective gating

III. TUBE VOLTAGE ADJUSTMENT

Dose is approximately proportional to the square of the tube voltage (kilovoltage, kV). Therefore, the tube current and tube voltage should be adjusted according to the patient size to optimize the patient dose. Reducing the tube voltage is effective for reducing the patient dose while maintaining a desired contrast-to-noise ratio (CNR) [12].

An example of a semi-automatic tube voltage adjustment tool is CARE kV (Siemens Healthineer), which automatically adjusts the optimal kV setting for each individual patient for a CT examination. Data from localizer radiographs are used for optimizing the tube voltage and tube current so that a user-chosen CNR is maintained with the lowest dose (Fig. 6). The tube voltage cannot be modulated during acquisition. A previous study demonstrated that the radiation dose and amount of contrast material could be reduced in abdominal dynamic CT without deteriorating the image quality [13].

However, changes in kV result in a change in X-ray photon energy, and changes in X-ray photon energy result in a change in tissue CT values. Therefore, variations in kV cause substantial changes in image contrast.

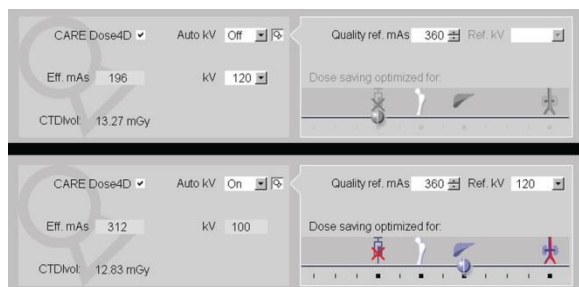


Fig. 6 Screen shot of the CARE kV (Siemens Healthineer) operation display. The tube voltage is adjusted according to the examination purpose selected by sliding the blue circle at the right lower part, “Dose saving optimized for”

IV. OPTIMIZING RECONSTRUCTION KERNEL

Reconstruction kernels themselves are not directly related to the patient dose, but the patient dose may be reduced by selecting an optimal reconstruction kernel. If high resolution kernels are used, image noise levels increase. If low resolution (smooth) kernels are used, image noise levels decrease without increasing the patient dose.

Iterative reconstruction (IR) is an algorithm for generating cross-sectional images from measured projections of an object. The algorithm has been applied to single-photon emission CT or positron emission tomography. In CT, this method was not used because of its significantly slower calculation speed than that of filtered back projection (FBP), which is the standard CT image reconstruction algorithm. However, various new image reconstruction systems that use IR algorithms have been recently developed. Using these systems, patient doses can be reduced while maintaining the image noise levels.

Although specific algorithms differ among manufacturers, the clinical basis for the benefits of IR implementation primarily involves reducing image noise levels, leading to improved objective and subjective image quality compared with those using FBP reconstructions [14]. However, IR techniques can result in the degradation of image quality by imparting an unfamiliar “plastic” texture to images that can interfere with the accuracy of diagnosis to an extent [15]. Another limitation is that computational power and time are required for IR. Delay between data acquisition and availability of images depends on the type of IR algorithm and the number of images.

Some third-party vendors have recently provided systems that are based on the IR approach. One example of these systems is SafeCT (Medic Vision, Tirat Carmel, Israel) (Fig. 7). It is a centralized network-based add-on system that can connect to any CT systems in an imaging department via digital imaging and communications in medicine network. Even if CT systems do not have image reconstruction systems that use IR algorithms, it can receive images from the CT console, automatically process them using IR algorithms, and transfer the processed images to the picture archiving and communication system for interpretation.

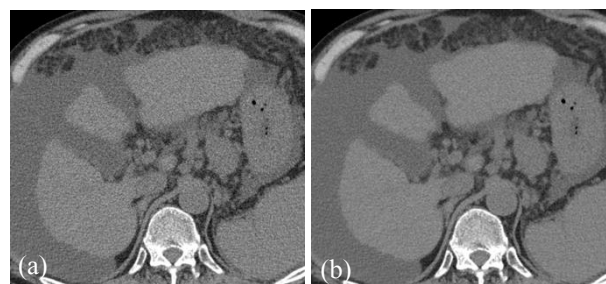


Fig. 7 An example of abdominal CT images before (a) and after (b) process using SafeCT (Medic Vision): The image noise levels decreased after process without deteriorating the spatial resolution

V. OPTIMIZING IMAGE SLICE THICKNESS

Images that have thin slice thicknesses can be easily obtained if MDCT systems are used. A thinner image thickness decreases the partial volume effect but increases image noise levels. To obtain thinner image thicknesses with lower image noise levels, higher radiation doses are required. However, CNR and visibility of small lesions can improve, despite increased noise levels when thinner slice thicknesses are used [16].

VI. OPTIMIZING BOWTIE FILTER

CT systems use bowtie filters to shape the X-ray beam and remove lower energy photons before the beam reaches the patient. The filter equalizes the radiation amount reaching the detector (Fig. 8).

In general, an optimal bowtie filter is selected when an optimal scan field of view is chosen. Therefore, operators should choose an optimal scan field of view according to the anatomical size and acquisition region of the patient.

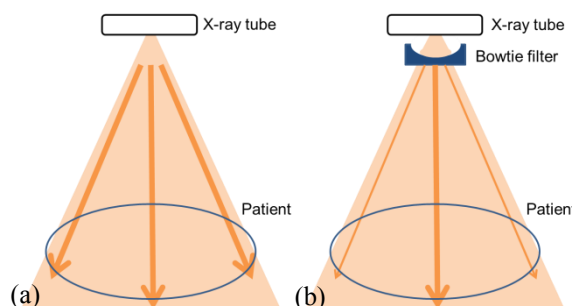


Fig. 8 Effectiveness of bowtie filter: (a) without a bowtie filter and (b) with a bowtie filter. The bowtie filter hardly absorbs X-rays at the center but absorbs off-axis X-rays to maintain a more uniform X-ray field at the detector

VII. OPTIMIZING NUMBER OF ACQUISITION PHASES

There is no doubt that the patient dose increases when the number of acquisition phases increases. However, optimizing the number of acquisition phases is not easy. For example, one study reported that the detectability of

hepatocellular carcinoma improved using four-phase CT image acquisitions [17], but another study reported that four-phase CT image acquisitions compared with three-phase CT image acquisitions did not improve the detection of hepatocellular carcinoma [18]. It is necessary for radiologists to keep in mind that the number of repetitions should be minimized.

VIII. APPLICATION OF SELECTIVE ORGAN SHIELDING

Selective organ shielding may be one of the choices for reducing the radiation dose in radiosensitive organs such as the breast, thyroid, and eye lens. A latex sheet that contains bismuth is generally used for this purpose. Fig. 9 shows an image of breast shielding that was achieved by applying a commercially available latex sheet over the breasts. The shield can attenuate many X-ray photons that would be absorbed by the breasts so that the absorbed dose in the breasts can be decreased.

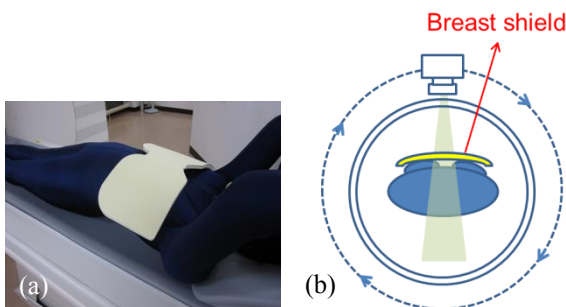


Fig. 9 Breast shielding: (a) placing a bismuth breast shield (AttenuRad ARB42; F&L Medical Products, Vandergrift, PA, USA) over the breasts and (b) illustration of breast shielding in CT

The use of selective organ shielding for pediatric and coronary calcium scoring CT has been recommended because the diagnostic image quality is not seriously affected by the shielding [19,20]; in contrast, shielding in thoracic CT has not been recommended because of its effect on CT numbers, artifacts, and image noise levels [21,22]. Therefore, judging whether selective organ shielding should be applied or not on the basis of the examination purpose is important.

If selective organ shielding is applied, some AEC systems that use at least one localizer radiograph to calculate the attenuation profile of the patient cannot correctly calculate the attenuation profile of the patient. Although the issue can be avoided by placing a shield after obtaining the localizer radiograph, the shield may prevent obtaining images with the quality required for the diagnosis. Other AEC systems that modulate the tube current according to the near-real-time attenuation data obtained from the previous 180° projection during the scan cannot correctly calculate attenuation data, even if the shield is placed over a radiosensitive organ after obtaining the localizer radiograph.

IX. APPLICATION OF DUAL-ENERGY CT

Radiation doses in dual-energy CT are similar to those in single-energy CT [23]. However, dual-energy CT allows the differentiation among multiple materials and the quantification of the mass density of two or three materials in a mixture with known elemental composition [24]. One of the examples that uses a three-material decomposition algorithm is a virtual non-contrast (VNC) image. This algorithm can remove iodine from contrast-enhanced CT images. If VNC images can be used instead of true non-contrast (TNC) images, TNC acquisition can be omitted to reduce the total patient dose. Previous studies showed that VNC images can replace TNC images for detecting or diagnosing a subarachnoid and intracranial hemorrhage, acute ischemia, liver lesion, hypoattenuating pancreatic lesion, hyperdense renal lesion, and urinary stones [25-30].

An example of abdominal dual-energy CT images before and after iodine subtraction is shown in Fig. 10. It is confirmed that iodine is removed from contrast-enhanced CT images to obtain VNC images. A previous phantom study revealed that VNC images provide reliable attenuation measurements for low, moderate, and high iodine-induced attenuations; however, for tissues with an extremely high iodine contrast agent load (e.g., excretory phase of CT urography), VNC values become less accurate and VNC attenuation increases over TNC attenuation because of beam hardening of X-rays [31].

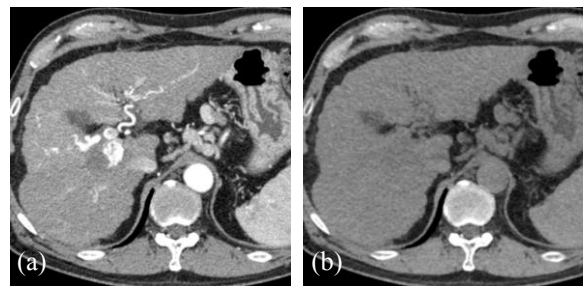


Fig. 10 Abdominal dual-energy CT images: (a) before iodine subtraction (contrast-enhanced image) and (b) after iodine subtraction (VNC image)

X. APPLICATION OF NEWLY DEVELOPED X-RAY DETECTION SYSTEM

CT basically uses scintillators such as cadmium tungstate to turn X-rays into light. The light is then converted into electrical signals using a photo diode. If the efficient of X-ray detection can be increased or electronic noise levels can be reduced in an X-ray detection system, further patient dose reduction is possible.

One manufacturer uses a new garnet gemstone material (Gemstone Detector; GE Healthcare, Milwaukee, WI, USA) as a scintillator. The advantage of the material includes high X-ray detection efficiency, and the gemstone-based scintillator can significantly reduce radiation doses [32].

Another manufacturer uses praseodymium-activated scintillator in their detector (^{PURE}VISION Detector; Toshiba

Medical Systems, Tochigi, Japan). Similar to the Gemstone Detector, its advantage is high X-ray detection efficiency.

A third manufacturer uses integrated CT detectors (Stellar and Stellar^{INFINITY} Detectors; Siemens Healthineer) that directly couples the photodiode with the analog-to-digital convertor to reduce the amount of electronic noise levels and artifacts [33], thereby reducing radiation doses.

XI. CONCLUSIONS

CT examinations are associated with substantially higher radiation exposure than conventional X-ray examinations, making radiation exposure from CT examinations a potential concern. In recent years, the news media, in addition to professionals, have focused on the potential risks of radiation exposure from CT examinations. In such situations, it is important for radiologists, physicists, and technologists to recognize the benefits and risks of CT examinations and follow ALARA principles by becoming familiar with available methods and techniques, described in this review, for optimizing patient dose in CT examinations. We hope that readers can optimize CT dose while maintaining diagnostic examination quality.

ACKNOWLEDGMENTS

We thank Dr. Slavik Tabakov, President of IOMP, for giving us the opportunity to submit our full paper on CT dose optimization to *Medical Physics International*. We also thank Mr. Nahomu Kameda of Nagase & Co., Ltd. and Mr. Eliran Dahan of Medic Vision for giving us the opportunity to use SafeCT.

This article includes results from studies supported by JSPS KAKENHI Grant Numbers 24791279 and 15K09887.

REFERENCES

- Rogers LF. (2001) Radiation exposure in CT: why so high? *AJR Am J Roentgenol* 177:277
- Brenner DJ, Elliston CD, Hall EJ, Berdon WE. (2001) Estimated risks of radiation-induced fatal cancer from pediatric CT. *AJR Am J Roentgenol* 176:289–296
- Donnelly LF, Emery KH, Brody AS, et al. (2001) Minimizing radiation dose for pediatric body applications of single-detector helical CT: Strategies at a large children’s hospital. *AJR Am J Roentgenol* 176:303–306
- Pearce MS, Salotti JA, Little MP, et al. (2012) Radiation exposure from CT scans in childhood and subsequent risk of leukaemia and brain tumours: a retrospective cohort study. *Lancet* 380:499–505
- Mathews JD, Forsythe AV, Brady Z, et al. (2013) Cancer risk in 680 000 people exposed to computed tomography scans in childhood or adolescence: data linkage study of 11 million Australians. *BMJ* 346:f2360
- Brooks RA, Di Chiro G (1976) Statistical limitations in x-ray reconstructive tomography. *Med Phys* 3:237–240
- Matsubara K, Koshida K, Ichikawa K, et al. (2009) Misoperation of CT automatic tube current modulation systems with inappropriate patient centering: phantom studies. *AJR Am J Roentgenol* 192:862–865
- Matsubara K, Sugai M, Toyoda A, et al. (2012) Assessment of an organ-based tube current modulation in thoracic computed tomography. *J Appl Clin Med Phys* 13:3731
- Doody MM, Lonstein JE, Stovall M, Hacker DG, Luckyanov N, Land CE (2000) Breast cancer mortality after diagnostic radiography: findings from the U.S. Scoliosis Cohort Study. *Spine* 25:2052–2063
- Wang J, Duan X, Christner JA, Leng S, Grant KL, McCollough CH (2012) Bismuth shielding, organ-based tube current modulation, and global reduction of tube current for dose reduction to the eye at head CT. *Radiology* 262:191–198
- Matsubara K, Koshida K, Noto K, et al. (2011) Estimation of organ-absorbed radiation doses during 64-detector CT coronary angiography using different acquisition techniques and heart rates: a phantom study. *Acta Radiol* 52:632–637
- Huda W, Scalzetti EM, Levin G (2000) Technique factors and image quality as functions of patient weight at abdominal CT. *Radiology* 217:430–435
- Nakayama Y, Awai K, Funama Y, et al. (2005) Abdominal CT with low tube voltage: preliminary observations about radiation dose, contrast enhancement, image quality, and noise. *Radiology* 237:945–951
- Geyer LL, Schoepf UJ, Meinel FG, et al. (2015) State of the art: iterative CT reconstruction techniques. *Radiology* 276:339–357
- Marin D, Nelson RC, Schindera ST, et al. (2010) Low-tube-voltage, high-tube-current multidetector abdominal CT: improved image quality and decreased radiation dose with adaptive statistical iterative reconstruction algorithm—initial clinical experience. *Radiology* 254:145–153
- Wedegärtner U, Yamamura J, Nagel HD, et al. (2007) Image quality of thickened slabs in multislice CT chest examinations: postprocessing vs. direct reconstruction. *Rofo* 179:373–379
- Murakami T, Kim T, Takamura M, et al. (2001) Hypervascular hepatocellular carcinoma: detection with double arterial phase multi-detector row helical CT. *Radiology* 218:763–767
- Kim SK, Lim JH, Lee WJ, et al. (2002) Detection of hepatocellular carcinoma: comparison of dynamic three-phase computed tomography images and four-phase computed tomography images using multidetector row helical computed tomography. *J Comput Assist Tomogr* 26:691–698
- Fricke BL, Donnelly LF, Frush DP, et al. (2003) In-plane bismuth breast shields for pediatric CT: effects on radiation dose and image quality using experimental and clinical data. *AJR Am J Roentgenol* 180:407–411
- Yilmaz MH, Yaşar D, Albayram S, et al. (2007) Coronary calcium scoring with MDCT: the radiation dose to the breast and the effectiveness of bismuth breast shield. *Eur J Radiol* 61:139–143
- Vollmar SV, Kalender WA (2008) Reduction of dose to the female breast in thoracic CT: a comparison of standard-protocol, bismuth-shielded, partial and tube-current-modulated CT examinations. *Eur Radiol* 18:1674–1682
- Kalra MK, Dang P, Singh S, Saini S, Shepard JA (2009) In-plane shielding for CT: effect of off-centering, automatic exposure control and shield-to-surface distance. *Korean J Radiol* 10:156–163
- Henzler T, Fink C, Schoenberg SO, Schoepf UJ (2012) Dual-energy CT: radiation dose aspects. *AJR Am J Roentgenol* 199:S16–S25
- McCollough CH, Leng S, Yu L, Fletcher JG (2015) Dual- and multi-energy CT: principles, technical approaches, and clinical applications. *Radiology* 276:637–665
- Zhang LJ, Peng J, Wu SY, et al. (2010) Liver virtual non-enhanced CT with dual-source, dual-energy CT: a preliminary study. *Eur Radiol* 20:2257–2264
- Quiney B, Harris A, McLaughlin P, Nicolaou S (2015) Dual-energy CT increases reader confidence in the detection and diagnosis of hypoattenuating pancreatic lesions. *Abdom Imaging* 40:859–864
- Jiang XY, Zhang SH, Xie QZ, et al. (2015) Evaluation of virtual noncontrast images obtained from dual-energy CTA for diagnosing subarachnoid hemorrhage. *AJNR Am J Neuroradiol* 36:855–860
- Cha D, Kim CK, Park JJ, Park BK (2016) Evaluation of hyperdense renal lesions incidentally detected on single-phase post-contrast CT using dual-energy CT. *Br J Radiol* 89:20150860
- Gariani J, Cuvincius V, Courvoisier D, et al. (2016) Diagnosis of acute ischemia using dual energy CT after mechanical thrombectomy. *J Neurointerv Surg* 8:996–1000

30. Bonatti M, Lombardo F, Zamboni GA, Pernter P, Pozzi Mucelli R, Bonatti G (2017) Dual-energy CT of the brain: Comparison between DECT angiography-derived virtual unenhanced images and true unenhanced images in the detection of intracranial haemorrhage. *Eur Radiol* 27:2690–2697
31. Toepker M, Moritz T, Krauss B, et al. (2012) Virtual non-contrast in second-generation, dual-energy computed tomography: reliability of attenuation values. *Eur J Radiol* 81:e398–e405
32. Geyer LL, Körner M, Harrieder A, et al. (2016) Dose reduction in 64-row whole-body CT in multiple trauma: an optimized CT protocol with iterative image reconstruction on a gemstone-based scintillator. *Br J Radiol* 89:20160003
33. Duan X, Wang J, Leng S, et al. (2013) Electronic noise in CT detectors: Impact on image noise and artifacts. *AJR Am J Roentgenol* 201:W626–W632

Contacts of the corresponding author:

Author: Kosuke Matsubara, Ph.D.
Institute: Kanazawa University
Street: 5-11-80 Kodatsuno
City: Kanazawa
Country: Japan
Email: matsuk@mhs.mp.kanazawa-u.ac.jp